International Journal of Power Electronics and Drive System (IJPEDS)
Vol. 8, No. 2, June 2017, pp. 558~583
ISSN: 2088-8694, DOI: 10.11591/ijpeds.v8i2.pp558-583

A Constant Switching Frequency DTC for PMSM Using Low Switching Losses SVM-An Experimental Result

K. Chikh[1], A. Saad[2], M. Khafallah[3], D. Yousfi[4], F.Z. Tahiri[5], M. Hasoun[6]
[1] Interdisciplinary Laboratory for Research in Science and Technology, Sultan Moulay Slimane University, Morocco
[2] Department of Electrical Engineering, Mohammed I University, Morocco
[2,3,5,6] Department of Electrical Engineering, Hassan II University, Morocco

Article Info

Article history:

Received Feb 13, 2017
Revised Apr 17, 2017
Accepted May 1, 2017

Keyword:

DTC
IP controller
PMSM
SVM
Switching frequency

ABSTRACT

A Constant Switching Frequency Direct Torque Control (CSF-DTC) with low switching losses Space Vector modulation (SVM) for Permanent Magnet Synchronous Motor (PMSM) drive is proposed in this work. The CSF-DTC combines Field Oriented Control (FOC) and basic DTC advantages. Indeed, the proposed control strategy improves the basic DTC performances, which features low flux and torque ripples as well as a fixed switching frequency. The improved DTC ensures also a fast and robust flux and torque responses by using Integral and Proportional (IP) controllers which guaranteed a good disturbance rejection.On the other hand, a symmetrical SVM technique with low switching losses in the PWM inverter is used in order to generate the desired stator voltage vector needed to control the stator flux and the motor torque. Simulation and experimental results are presentedin this paper.These results demonstrate well the performance of the basic and proposed DTC and they show the effectiveness of the constant switching frequency direct torque control.

Copyright © 2017 Institute of Advanced Engineering and Science.
All rights reserved.

Corresponding Author:

Khalid Chikh,
Department of Electrical Engineering,
Sultan Moulay Slimane University,
Ecoe superieure de technologie, BP591, 23000, Béni mellal, Marocco.
Email: genielectrique@gmail.com

1. INTRODUCTION

Today Field Oriented Control (FOC) and Direct Torque Control (DTC) are considered the most important techniques to achieve high dynamic performance in AC machines [18]. DTC technique has been first proposed and applied for induction machines in the mid-1980s, by Takahachi and Noguchi, for low and medium power applications [9]-[14]. The basic idea of DTC for an induction motor is to control the torque and flux linkage by selecting the voltage space vectors properly, which is based on the relationship between the slip frequency and torque [18]. This concept can also be applied to synchronous drives [10].

Indeed, DTC technique for PMSM has appeared in the late 1990s as reported in [8]-[9]. However, for some applications, the DTC has become unusable although it significantly improves the dynamic performance (fast torque and flux responses) of the drive and is less dependent on the motor parameters variations compared to the classical vector control (FOC) due to torque and flux ripples [7]-[8]. Indeed, hysteresis controllers used in the conventional structure of the DTC generates a variable switching frequency, causing electromagnetic torque oscillations. Also this frequency varies with speed, load torque and hysteresis bands selected. In addition, a high sampling frequency is needed for digital implementation of hysteresis comparators and a current and torque distortion is caused by sectors changes [6].In the last decade, several contributions have been proposed to overcome these problems :

a. By matrix converter [23] or also by changing de switching Table [1, 4, 11].

b. By combining basic DTC and fuzzy logic control in one control strategy, named fuzzy direct torque control [8].
c. By replacing the hysteresis controllers and the switching table by a PI regulator, predictive controller and SVM [6, 7, 9, 10, 14].

In the modified DTC, proposed in these works, at least one of the propertiesbellow is needed to achieve a lower torque and flux ripple:

a. More power switches.
b. Variable switching frequency.
c. Increase of the system cost and/or complexity.

This paper proposes a modified DTC algorithm for PMSM drive in order to reduce the flux and torque ripples. But, at the same time this control strategy is characterized by:

a. Low switching losses and fixed constant switching frequency by using a symmetrical SVM.
b. Good speed, torque and flux dynamic state by using the IP controllers.
c. Simple algorithm.

The basic DTC and the proposed DTC algorithms were investigated by simulations under Matlab/Simulink and then experimentally using dSPACE 1104 board. In order to show the superiority of the proposed DTC strategy, the sampling time used to investigate the standard DTC, in simulation and in practice, is smaller than that used to investigate the proposed DTC algorithm. Also, these control strategies were compared at different operating conditions, namely: no load, speed tracking and disturbance rejection (load torque). Indeed, both simulation and experimental results show that our proposed DTC algorithm is more performant than classical DTC in all the cited operating conditions.

2. BASIC DTC FOR PMSM DRIVE

DTC is a vector control method used to control the torque and therefore the speed of the motor by controlling the switching sequence of the inverter transistors. The Figure 1 shows the basic DTC principle.

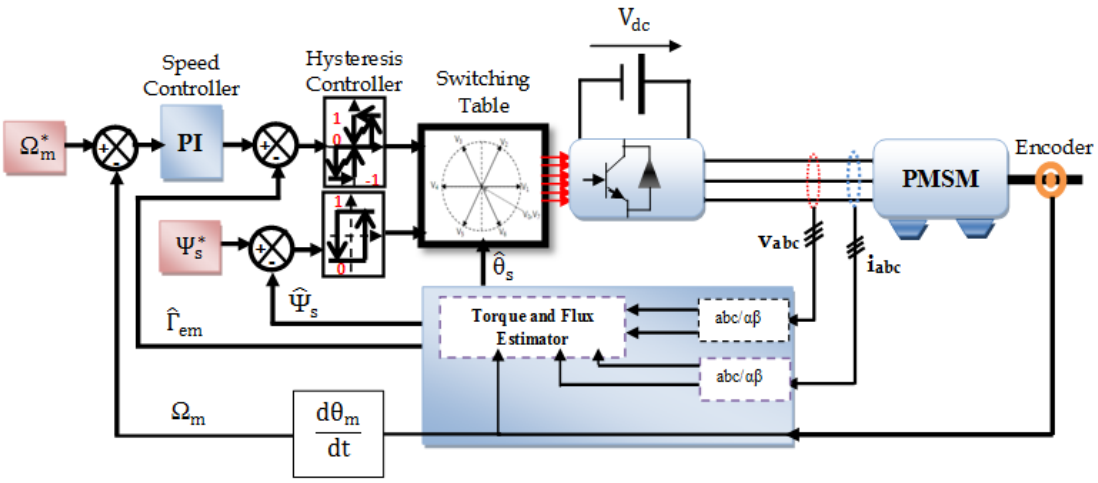

Figure 1. Basic DTC scheme for PMSM drive with speed loop

In the DTC, the motor torque control is achieved with two hysteresis controllers, one for stator flux magnitude error and the other for the torque magnitude error. The selection of one switching vector per sampling time depends on the sign of these two controllers without inspections of the magnitude of the errors produced in the transient and dynamic situations per sampling time and level of the applied stator voltage.

2.1. Stator Flux Control

The stator voltage vector equation, in a stator reference frame, is given by :

$$\bar{V}_s = R_s.\bar{I}_s + \frac{d\bar{\Psi}_s}{dt} \quad (1)$$

Where $\bar{V}_s = V_{s\alpha} + jV_{s\beta}$

$$\text{So } \bar{\Psi}_s = \bar{\Psi}_o + \int_0^t (\bar{V}_s - R_s.\bar{I}_s)\, dt \quad (2)$$

For high speeds, the term $R_s.\bar{I}_s$ can be neglected, so the equation 2 is given by:

$$\bar{\Psi}_s \approx \bar{\Psi}_o + \int_0^t \bar{V}_s\, dt \quad (3)$$

During the same sampling time T_e the selected stator voltage vector is always constant, Equation 3 becomes:

$$\bar{\Psi}_s(k+1) \approx \bar{\Psi}_s(k) + \bar{V}_s.T_e \quad (4)$$

$$\text{Or as } \Delta\bar{\Psi}_s = \bar{V}_s.T_e = \bar{\Psi}_s(k+1) - \bar{\Psi}_s(k) \quad (5)$$

With: $\bar{\Psi}_s(k)$ is the stator flux vector at the actual sampling time.
$\bar{\Psi}_s(k+1)$is the stator flux vector at the next sampling time.
$\Delta\bar{\Psi}_s$is the variation of stator flux vector.

From Equation 5, it is seen that the variation of the stator flux is directly proportional to the stator voltage; consequently the control is carried out by varying the stator flux vector by selecting a suitable voltage vector with the Voltage Source Inverter (VSI).

Figure 2 shows that the stator flux vector is varied in the same direction as the applied stator voltage vector. Therefore, applied a collinear stator voltage vector as the stator flux vector and in the same direction as it is a sufficiently condition to increase it, and vice versa.Indeed, to control the stator flux vector $\bar{\Psi}_s(k)$an estimator of its module $\hat{\Psi}_s$and its argument $\hat{\theta}_s$ is needed.

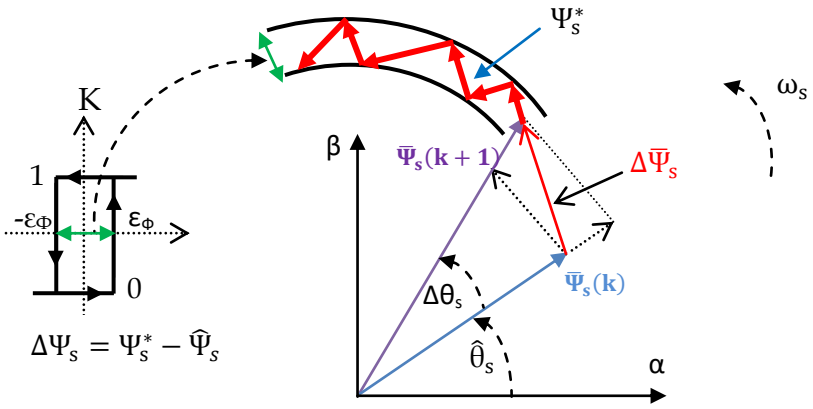

Figure 2. Stator flux vector evolution in the αβ subspace

The stator flux can be estimated from the measure of stator currents and voltages and their transformation in the αβ subspace, by integrating of difference between the input voltage and the voltage drop across the stator resistance as given by :

$$\Psi_\alpha = \Psi_m + \int_0^t (V_\alpha - R_s.I_\alpha)\, dt \quad (6)$$

$$\Psi_\beta = \int_0^t (V_\beta - R_s.I_\beta)\, dt \quad (7)$$

From Equations 6 and 7, the stator flux module and its argument are given by:

$$\hat{\Psi}_s = \sqrt{{\Psi_\alpha}^2 + {\Psi_\beta}^2} \quad (8)$$

$$\hat{\theta}_s = \text{Arc}\tan(\frac{\Psi_\beta}{\Psi_\alpha}) \quad (9)$$

A two level hysteresis controller, as indicated in figure 1, is used to control the stator flux, which compares the reference stator flux Ψ_s^* with the estimated stator flux$\hat{\Psi}_s$. The flux hysteresis comparator output is denoted by Boolean variable K_Ψ which indicates directly if the amplitude of flux must be increased $K_\Psi = 1$ or decreased $K_\Psi = 0$: if $K_\Psi = 1$, it means that the actual value of the flux linkage is below the reference value and outside the hysteresis limit; so the stator flux must be increased, while if $K_\Psi = 0$, it means that the actual value of the flux linkages is above the reference value and outside the hysteresis limit; so the stator flux must be decreased.

The two levels VSI, as shown in Figure 1, is used to select proper voltage vectors from the output of flux and torque hysteresis controller (will be presented in the next part). The inverter has eight permissible switching states (V_0, V_1 … V_7), out of which six are active (V_1, V_2… V_6) and two zero or inactive states (V_0 and V_7). The voltage vector plane is divided into six sectors so that each voltage vector divides each region in two equal parts as shown in Figure 3. In each sector four of the six non-zero voltage vectors along with zero vectors may be used.

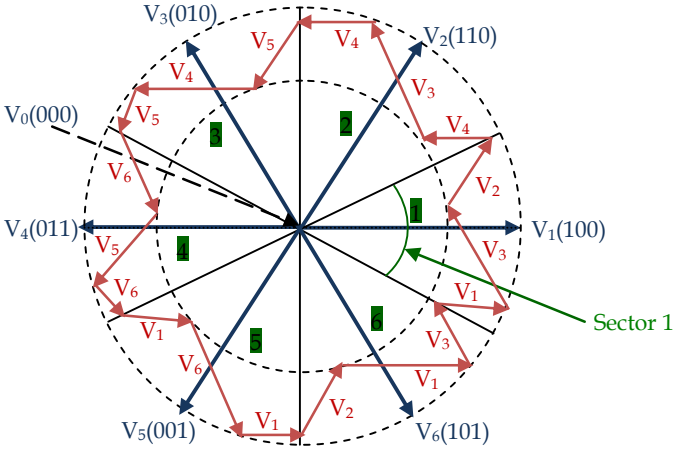

Figure 3. Control of stator flux by selection of the suitable voltage vector $V_{i(i=0,\ldots,7)}$

2.2. Electromagnetic Torque Control

The electromagnetic torque equation is defined as follows :

$$\Gamma_{em} = k.(\bar{\Psi}_s.\bar{\Psi}_r) = \|\bar{\Psi}_s\|.\|\bar{\Psi}_r\|.\sin\delta \quad (10)$$

Where δ is the angle between the rotor and the stator flux vectors and the constant k is expressed as (when $L_d = L_q$):$k = \frac{3P}{2L_q}$. The Equation 10 indicates that the electromagnetic torque depends to the rotor and stator amplitude, and the angle δ. So, if the stator flux vector is perfectly controlled, by mean of the stator voltage vector$\bar{V}_s$, in module and in position; consequently, the electromagnetic torque can be controlled by the same stator voltage vector.

Note that the electromagnetic torque can be controlled by mean of a two level comparator as the same as stator flux (see Figure 3) or by using a three level comparator as shown in Figure 4. In this work, a three level comparator has been used in order to minimize the switches commutation numbers and to have the two senses of the motor rotation. The output of this controller is represented by a Boolean variable $K_T$which indicates directly if the amplitude of the torque must be increased, maintained constant or decreased, respectively, when K_T is equal 1, 0 or -1. The goal of this controller is to maintain the torque variation $\Delta\Gamma_{em}$ in the bandwidth [$-\varepsilon_T$,ε_T] chosen by the programmer of DTC algorithm. Indeed, this controller adjusts the torque variation generated by a comparator of electromagnetic torque reference (Γ_{em}^*)and the estimated torque ($\hat{\Gamma}_{em}$).

$$\Delta\Gamma_{em} = \Gamma_{em}^{*} - \hat{\Gamma}_{em} \quad (11)$$

The torque can be estimated by using the Equation:

$$\hat{\Gamma}_{em} = \frac{3}{2}P\left[\Psi_{\alpha}I_{\beta} - \Psi_{\beta}I_{\alpha}\right] \quad (12)$$

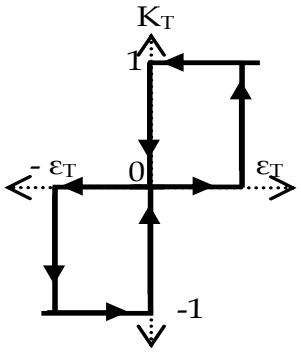

Figure 4. Three level hysteresis controller

2.3. Switching Table for Controlling Flux and Torque

According to the signal generated by the hysteresis controller of stator flux and electromagnetic torque presented in Figure 3 and 5, respectively; just one voltage vector can be selected to adjust the torque and flux. The choice of this vector depends on the outputs of the torque and flux controller and the position of the stator flux vector, as shown in Table 1.

Table 1. Takahashi and Noguchi Switching Table

K_Ψ	K_T	θ_1	θ_2	θ_3	θ_4	θ_5	θ_6
	1	V_2	V_3	V_4	V_5	V_6	V_1
1	0	V_7	V_0	V_7	V_0	V_7	V_0
	-1	V_6	V_1	V_2	V_3	V_4	V_5
	1	V_3	V_4	V_5	V_6	V_1	V_2
0	0	V_0	V_7	V_0	V_7	V_0	V_7
	-1	V_5	V_6	V_1	V_2	V_3	V_4

2.4. Speed IP Controller Design

Figure 5 shows the block diagram of the IP speed controller. From this figure, the Equation bellow can be obtained:

$$w_m = \frac{1}{1+\frac{f+k_T k_{pv}}{k_T k_{pv} k_{iv}}s+\frac{J}{k_T k_{pv} k_{iv}}s^2} w_m^{*} - \frac{\frac{1}{k_T k_{pv} k_{iv}}s}{1+\frac{f+k_T k_{pv}}{k_T k_{pv} k_{iv}}s+\frac{J}{k_T k_{pv} k_{iv}}s^2}\Gamma_r \quad (13)$$

This transfer function in regulation mode doesn't have a zero contrary to that of the classical PI speed controller. In fact, the IP controller allows ensuring a good dynamic and steady states in tracking or regulation mode in spite of the torque load variation (disturbance). Indeed, the proportional and integral gains can be expressed as:

$$\begin{cases} k_{iv} = \frac{J\omega_n^2}{2\xi J\omega_n - f} \\ k_{pv} = \frac{2\xi J\omega_n - f}{k_T} \end{cases} \quad (14)$$

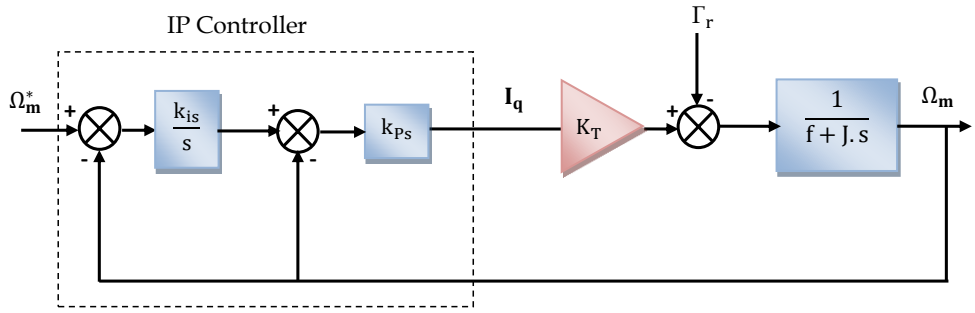

Figure 5. Closed loop speed using IP controller

3. Proposed DTC for PMSM drive

The block diagram of the proposed DTC-SVM for a voltage source PWM inverter fed PMSM is presented in Figure 6. In this modified DTC, torque and flux hysteresis controllers and the switching Table used in basic DTC are replaced by a two IP torque and flux controllers and a Space Vector PWM technique.

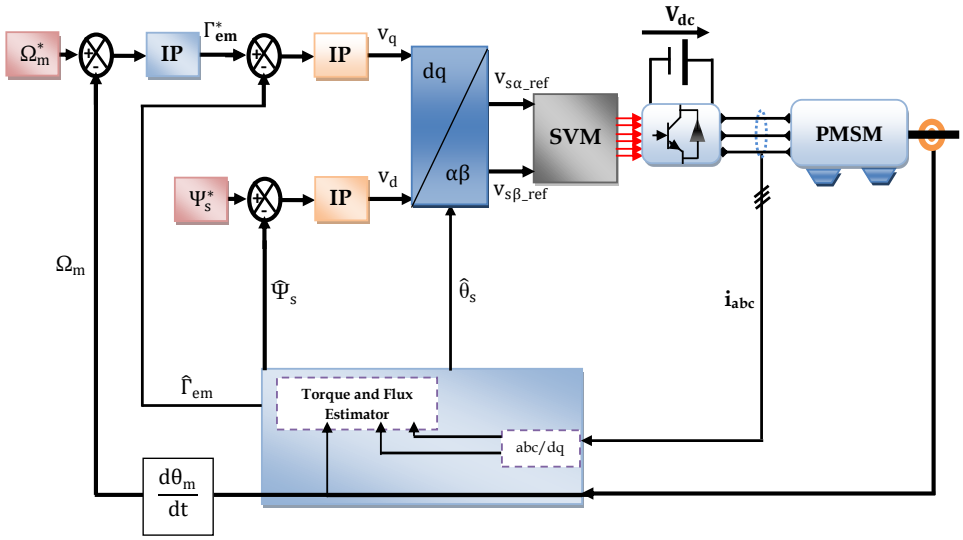

Figure 6. Proposed DTC-SVM scheme

3.1. PMSM model in d-q frame

The dynamic model of the PMSM in the rotor oriented coordinate d-q can be presented by the following Equations 15 and 16:

$$\begin{cases} v_d = R_s I_d + \frac{d\Psi_d}{dt} - w_s \Psi_q \\ v_q = R_s I_q + \frac{d\Psi_q}{dt} + w_s \Psi_d \end{cases} \quad (15)$$

$$\begin{cases} \Psi_d = L_d I_d + \Psi_m \\ \Psi_q = L_q I_q \end{cases} \quad (16)$$

The electromagnetic torque equation in the rotor oriented coordinate d-q can be expressed as:

$$\Gamma_{em} = \frac{3}{2} p\left(\Psi_d . I_q - \Psi_q . I_d\right) \quad (17)$$

Finally the motion Equation is given by:

$$\Gamma_{em} - \Gamma_r - f.w_m = J\frac{dw_m}{dt} \quad (18)$$

According to the Equations 14 and 15, if the stator flux vector is oriented along the d axis; Ψqbecomes equal to zero and the electromagnetic torque is a function of stator flux linkage Ψs and the q-axis current Iq. So if a fast dynamics flux control loop is imposed compared to the torque control loop; this last would be a direct function of the Iqcurrent component. In these conditions, the Equation 13 shows that the torque can be controlled throughthe q-axis voltage component Vqand the stator flux via the d-axis voltage component Vd.

3.2. Stator flux control

Figure 7 shows that when the stator flux is oriented along the d-axis, the d-axis flux component is directly proportional to the current I_d andq-axis flux component becomes zero. Therefore, by controlling and keeping constant the d-axis component of the stator current a decoupled flux and torque control can be obtained.

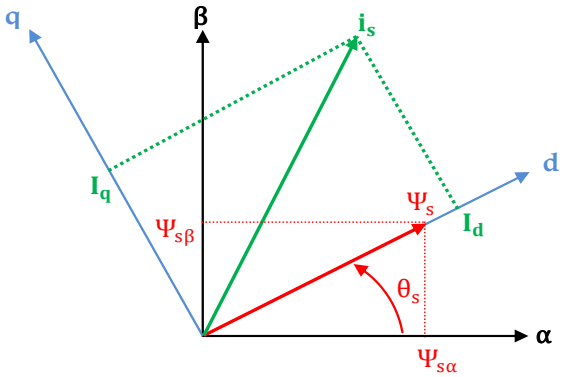

Figure 7. Vector diagram of the stator flux orientation strategy

According to the proposed DTC-SVM control strategy, the stator flux closed loop is represented in the Figure 7.

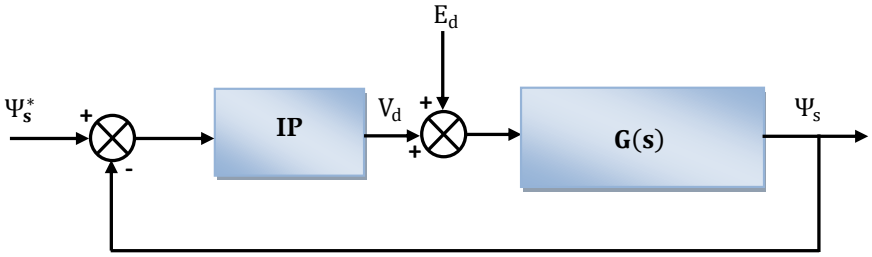

Figure 8. Closed loop stator flux using IP controller

Where G(s) isthe opened loopstator flux transfer function and Ed is constant disturbance. They are given by the Equations:

$$\begin{cases} G(s) = \frac{1}{\frac{R_s}{L_d} + s} \\ E_d = \frac{R_s}{L_d}\Psi_m \end{cases} \quad (19)$$

The closed loop flux transfer function is expressed as:

$$T(s) = \frac{\Psi_s}{\Psi_s^*} = \frac{1}{1+(K_{if}+\frac{R_s}{K_{if}K_{pf}L_d})s+\frac{1}{K_{if}K_{pf}}s^2} = \frac{1}{1+\frac{2\xi}{\omega_n}s+\frac{s^2}{\omega_n^2}} \quad (20)$$

We get by identification :

$$\begin{cases} K_{if} = \frac{L_d\omega_n^2}{2\xi L_d\omega_n - R_s} \\ K_{pf} = 2\xi\omega_n - \frac{R_s}{L_d} \end{cases} \quad (21)$$

3.3. Torque control

The electromagnetic torque closed loop by using an IP controller is represented in the Figure 9.

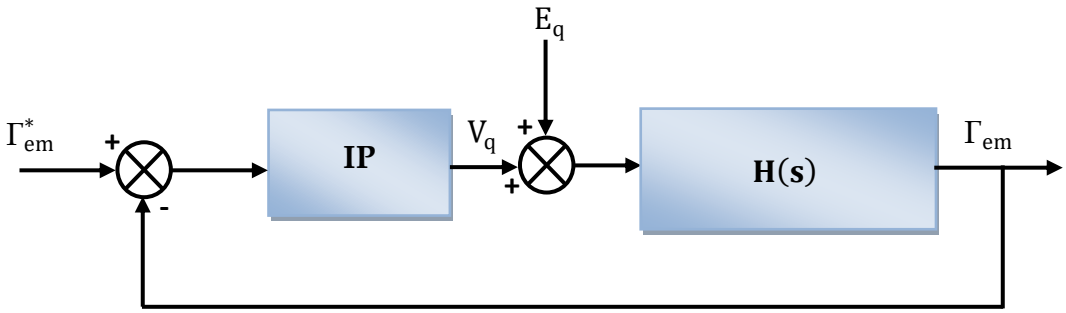

Figure 9. Closed loop electromagnetic torque using IP controller

Where:

$$\begin{cases} H(s) = \frac{\frac{3}{2}p\Psi_s}{R_s+L_qs} \\ E_q = -w_s\Psi_s \end{cases} \quad (22)$$

The closed loop torque transfer function is expressed as:

$$\frac{\Gamma_{em}}{\Gamma_{em}^*} = \frac{1}{1+\frac{R_s+K_TK_{pc}}{K_TK_{pc}K_{ic}}s+\frac{L_q}{K_TK_{pc}K_{ic}}s^2} \quad (23)$$

We get by identification:

$$\begin{cases} K_{pc} = \frac{2\xi L_q\omega_n - R_s}{K_T} \\ K_{ic} = \frac{L_q\omega_n^2}{2\xi L_q\omega_n - R_s} \end{cases} \quad (24)$$

3.4. Space Vector Modulation

The SVM block is used to generate the stator voltage vector V_s, needed to control theelectromagnetic torque and the stator flux in the CSF-DTC strategy, through the voltage source inverter.It's known that the inverter states can be considered to be voltage vectors and can be plotted on a state map as shown in Figure 9. In each sampling time, these vectors will be used to generate the V_s vector can be given by the following Equation:

$$V_s = \frac{1}{T_s}\left[\left(\frac{T_1}{2}V_1 + \frac{T_2}{2}V_2 + \frac{T_0}{2}V_0\right) + \left(\frac{T_0}{2}V_0 + \frac{T_2}{2}V_2\frac{T_1}{2}V_1\right)\right] \quad (25)$$

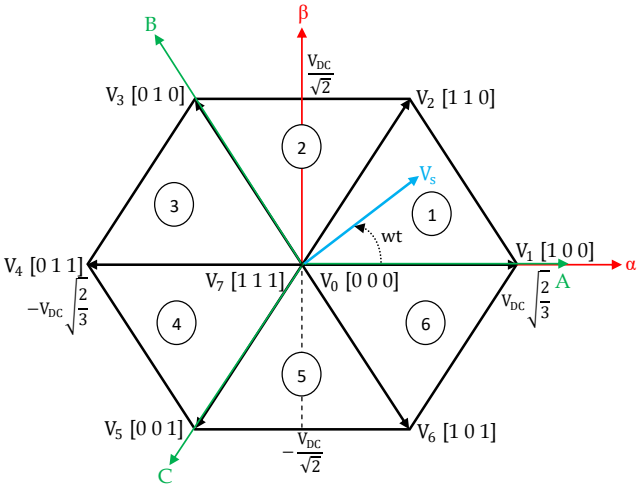

Figure 10. SVM state map and switching sequence

In the literature there are different SVM techniques due to the switching sequence choice. In fact, the choice of the null vector determines the SVM technique and it affects the phase waveform which affects inverter operation and inverter power losses.The popular SVM technique presented in the most papers is also the same technique used in DS1104 card. This technique is presented in Figure 10.b can be called symmetrical SVM. It's seen that this technique is to alternate the null vector in each sequence and reverse the sequence after each null vector, all that in each modulation period T_m [7, 20]. However, with this sequence strategy the 3 legs inverter are in commutation which generates 8 switching states in each T_m.

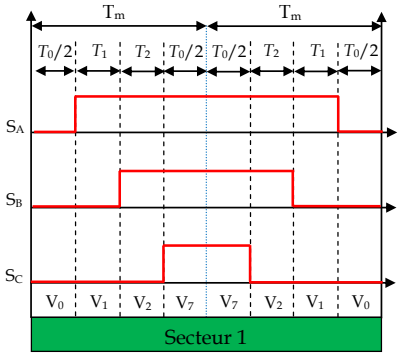

Figure 11a. Asymmetrical SVM

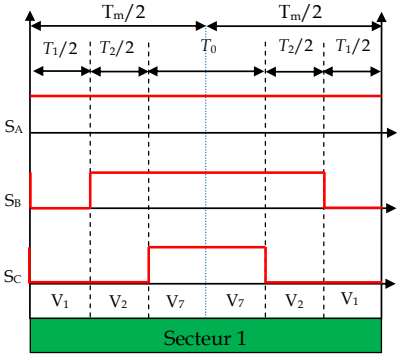

Figure 11b. Symmetrical SVM

Figure 11. Time sequences and applications of adjacent vectors in the first sector

In order to reduce the power inverter losses, we propose in this work a novel SVM technique whichguaranteed a good phase waveform and just 2 legs inverter will be in commutation in each modulation period as shown in Figure 10a. So, just 6 switching states will be generated. this SVM sequence strategy can be called asymmetrical SVM because it does not presents symmetry relative to the modulation period midpoint.

4. SIMULATION RESULTS

The models of the PMSM, voltage inverter, basic DTC algorithm and proposed DTCwith the asymetrical SVM algorithmsare developed in Matlab/Simulink in order to examine and to compare the complete behavior of these two strategies stydied in this paper.The switching delays and the forward drop of

the power switches, the dead time of the inverterand the nonideal effects of the PM machine are all neglected in the models. The PMSM parameters used in this work are shown in Table 2.

Table 2.The PMSM parameters values

Rated output power (Watt)	Rated phase voltage (Volt)	Magnetic flux linkage (Wb)
500	190	0.052
Rated torque (Nm)	Rated speed (rpm)	Maximum speed (rpm)
0.8	1000	6000
d-axis inductance (mH)	q-axis inductance (mH)	Inertia (Kg.m^2)
3.3	3.3	0.003573
Poles	Stator resistance (Ω)	friction coefficient (Nm.s/rd)
3	1.59	0.00047

Various tests at different operating conditions have been carried out, in Matlab/Simulink environment, in order to investigate the PMSM drive performances by using classical and proposed DTC. For this reason, the sampling time is 50µs (20 kHz) for the basic DTC and 100 µs (10 kHz) for the modified DTC. Note that this choice have real influence on the switching frequency and the torque and flux ripples, mainly in case of the basic DTC.To examine and to compare the robustness of these two strategies, a same operation of speed and load torque variation was applied to control the PMSM.

The simulation results of basic DTC and CSF-DTCare presented in Figure 12 and 13, respectively. As shown in Figures 12 and 13, it's seen that the stator flux and torque ripples are greatly reduced under the proposed DTC, in spite of the smaller samling time used to simulate the classical DTC. Also a high current distorsion can be observed in Figure 12f when compared to Figure 13f. This is mainly because in SVM algorithm, contrary to hysterisis controller and the switching table, the switching frequency is constant and also, in SVM, many vectors (IGBT states) are selected to adjust the torque and flux ripple in each sampling time, whereas in basic DTC just one vector is selected to adjust ripple inside hysteresis bands of torque and flux regulators.

In brief,the steady state performance of the CSF-DTC is much better than that of the basic DTC, in one hand. In the other hand, the same torque and flux dynamic state can be observed, expect the small delay in the flux at the start-up of the motor (see Figure 14). Figures 15 shows the stator phase current spectrums under the basic and modified DTC. Indeed, the current spectral analysis presented in Figure 15a shows that the Total Harmonic Distortion (THD) of the current waveform under basic DTC is 11.1 % whereas the THD of the current waveform of DTC-SVM is 3.35 %, it is smoother than that of the basic DTC. This is mainly due to the fact that the switching function of the inverter is only updated at the sampling instant and also the number of vectors applied to adjust the torque and flux ripple.

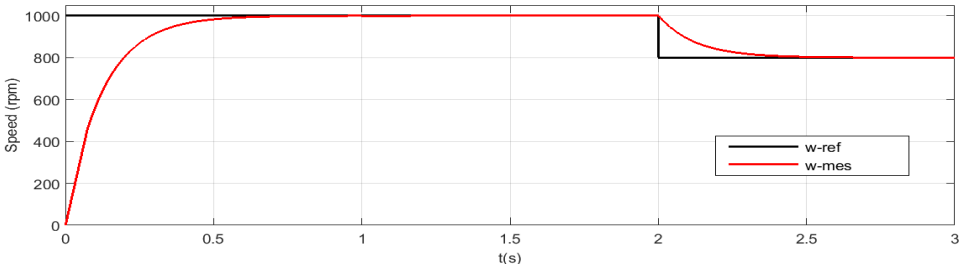

Figure 12a. Reference (w-ref) and measured speed (w-mes)

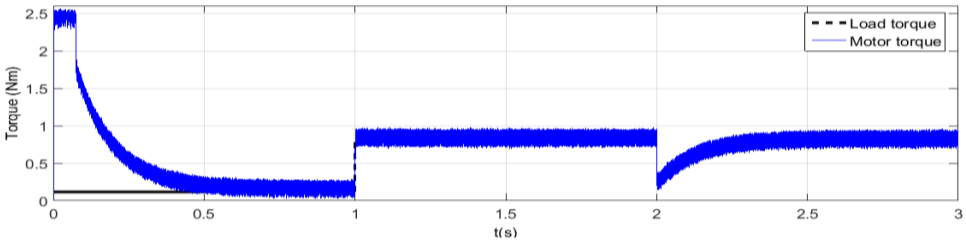

Figure 12b. Load torque and motor torque

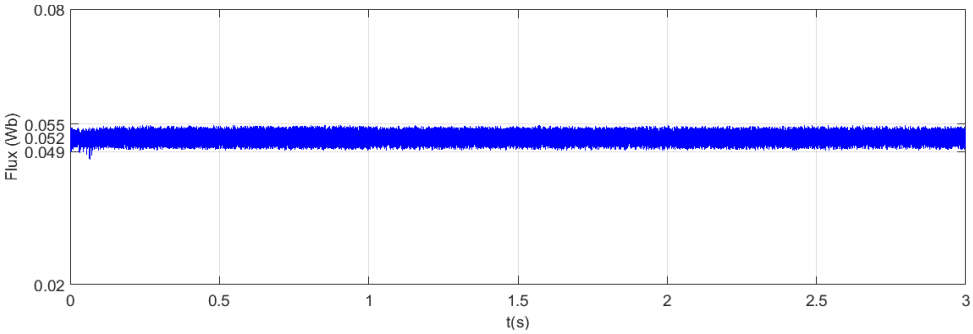

Figure 12c. Estimated stator flux linkage

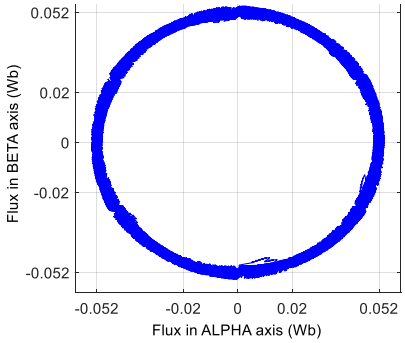

Figure 12d. Estimated stator flux vector components in (α,β) axis

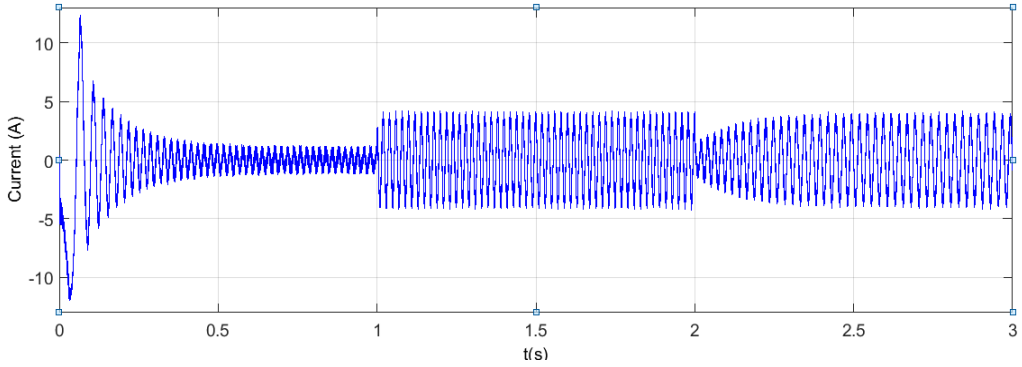

Figure 12e. Measured phase stator current

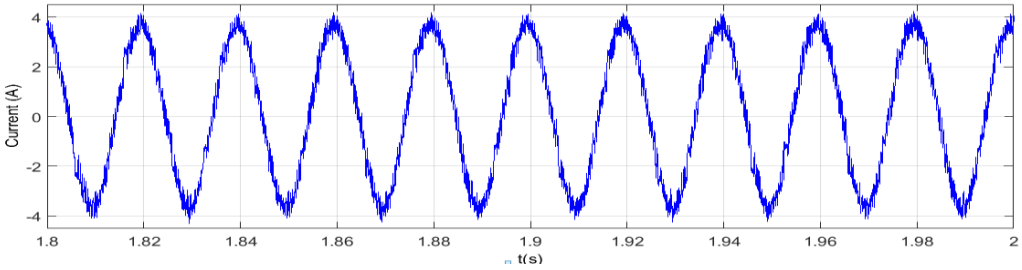

Figure 12f. Zoom in measured phase current

Figure 12. Simulation results of the basic DTC performance under speed and load torque variations

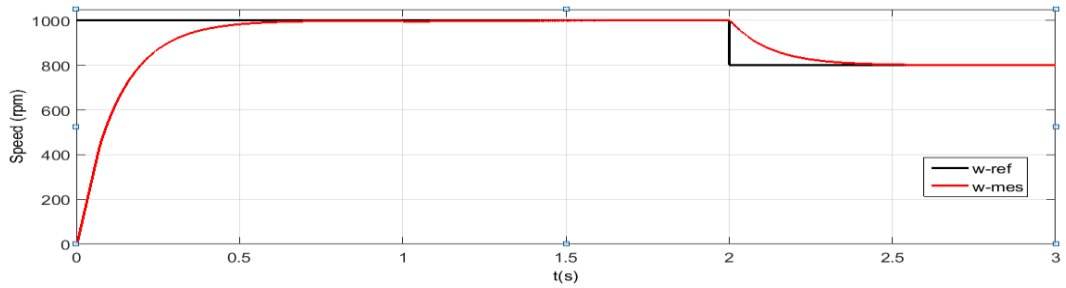

Figure 13a. Reference (w-ref) and measured speed (w-mes)

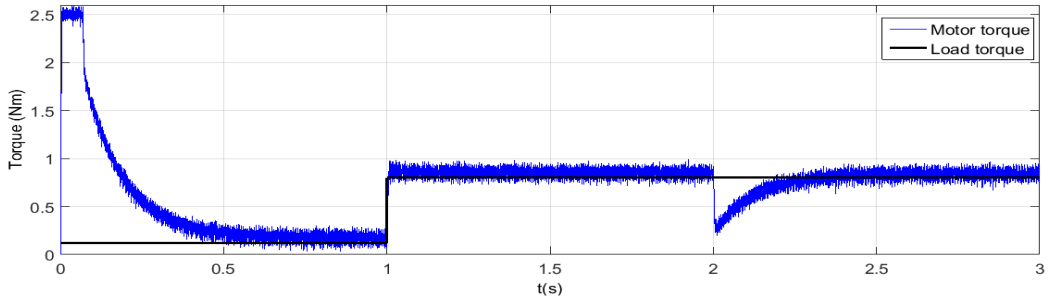

Figure 13b. Load torque and motor torque

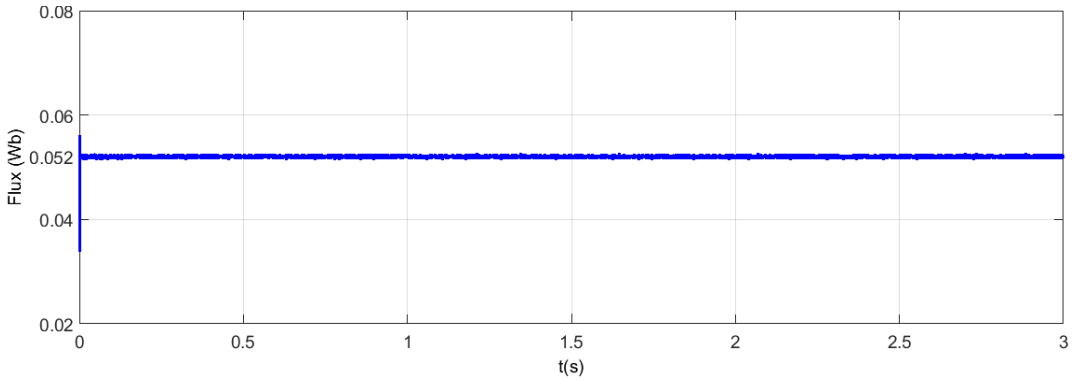

Figure 13c. Estimated stator flux linkage

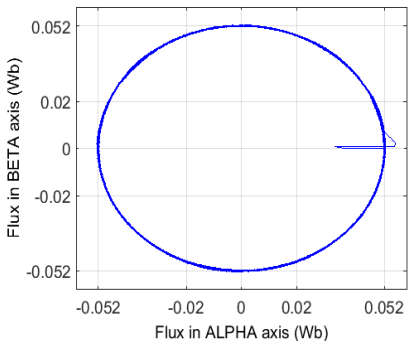

Figure 13d. Estimated stator flux vector components in (α,β) axis

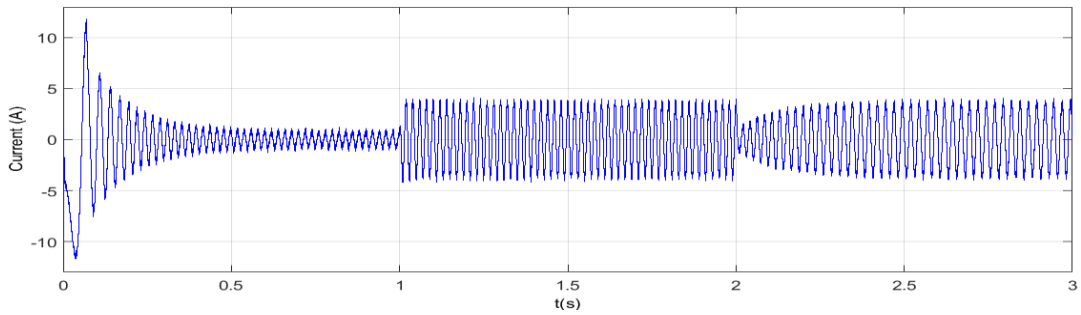

Figure 13e. Measured phase stator current

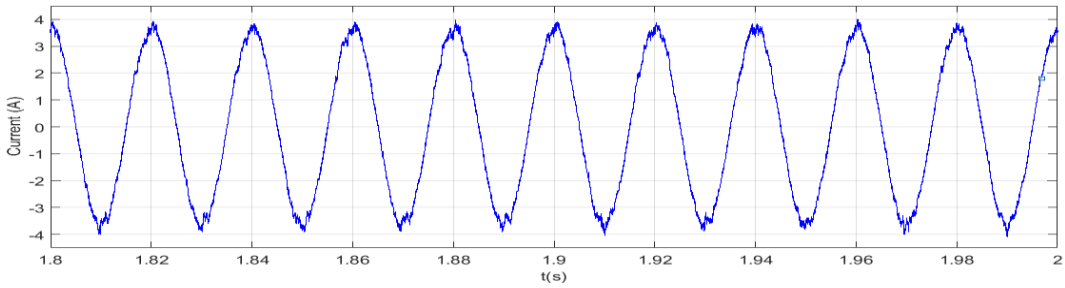

Figure 13f. Zoom in measured phase current

Figure 13. Simulation results of the Proposed CSF-DTC performance under speed and load torque variations

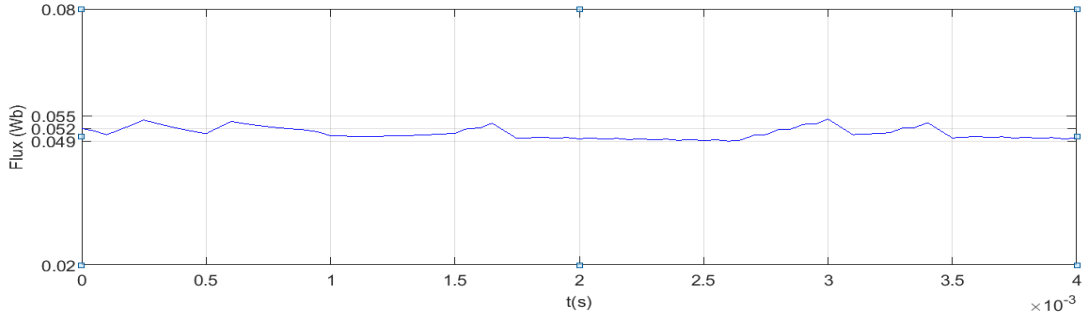

Figure 14a. DTC

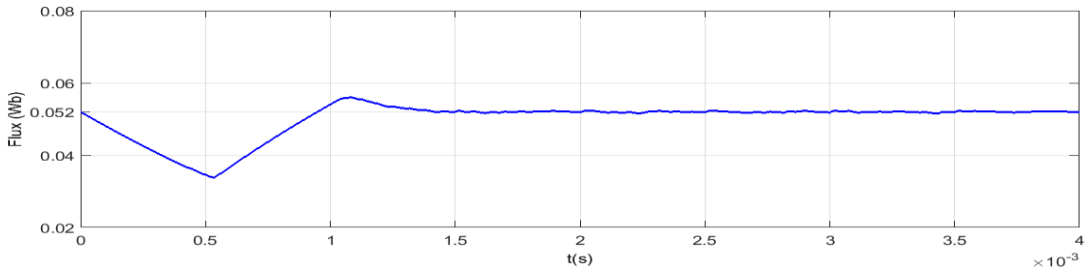

Figure 14b. Proposed CSF-DTC

Figure 14. Simulation results, stator flux dynamic state in case of basic DTC and proposed CSF-DTC

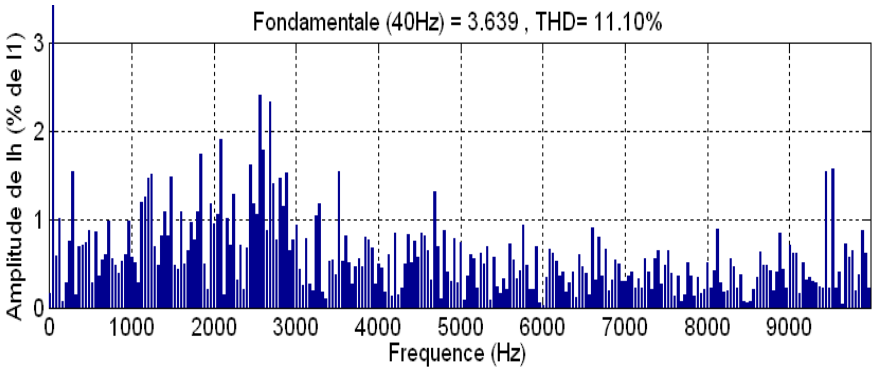

Figure 15a. Reference (w-ref) and measured speed (w-mes)

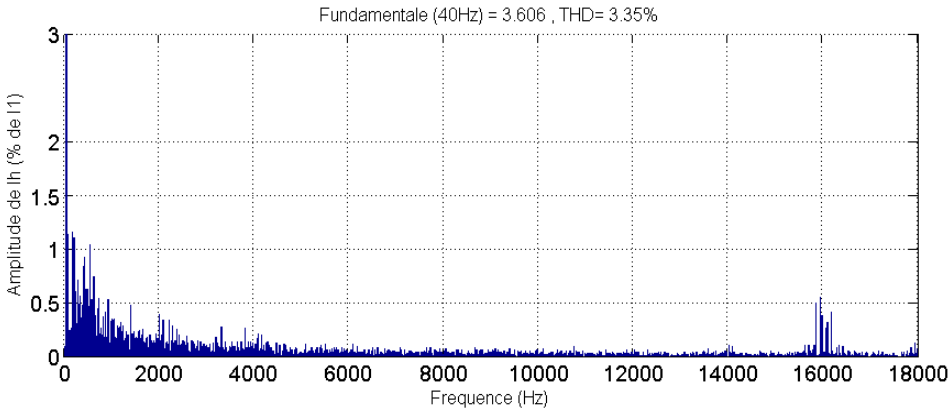

Figure 15b. Load torque and motor torque

Figure 15. Simulation results of the basic DTC performance under speed and load torque variations

5. EXPERIMENTAL RESULTS

A test bench was constructed, as indicated in Fgiure 16, in order to validate the simulation results of the DTC algorithms presented in this paper. Indeed, the Figure 16 shows that the IGBT inverter and the dSPACE DS1104 cardare used to drive the PMSM under test (whose pertinent parametres are given in Table 1). This motor is coupled to a separately excited DC generator. This later supplies a resistive bank, used to produce differents load torques. The DSP card is plugged in the PC and its equiped by a Matlab (to program the DSP card) and ControlDesk (to supervise the system) software.

The DS1104 digital signal processing DSP card is used to carry out the real-time algorithms, this system is based on PowerPC 603e microprocessor (main processor) running at 250 MHz (CPU clock) on wich the DTC algorithms were implemented and TMS320F240 DSP of Texas Instruments running at 20 MHz can be used to provides Space Vector Modulation, but in our case switching table ans SVM are generated by the main processor.The board is equipped with analog-to-digital converters for current and voltage sensors, digital-to-analog converters and an input for an incremental encoder how is used to detect the initial rotor position and the actual rotor speed.

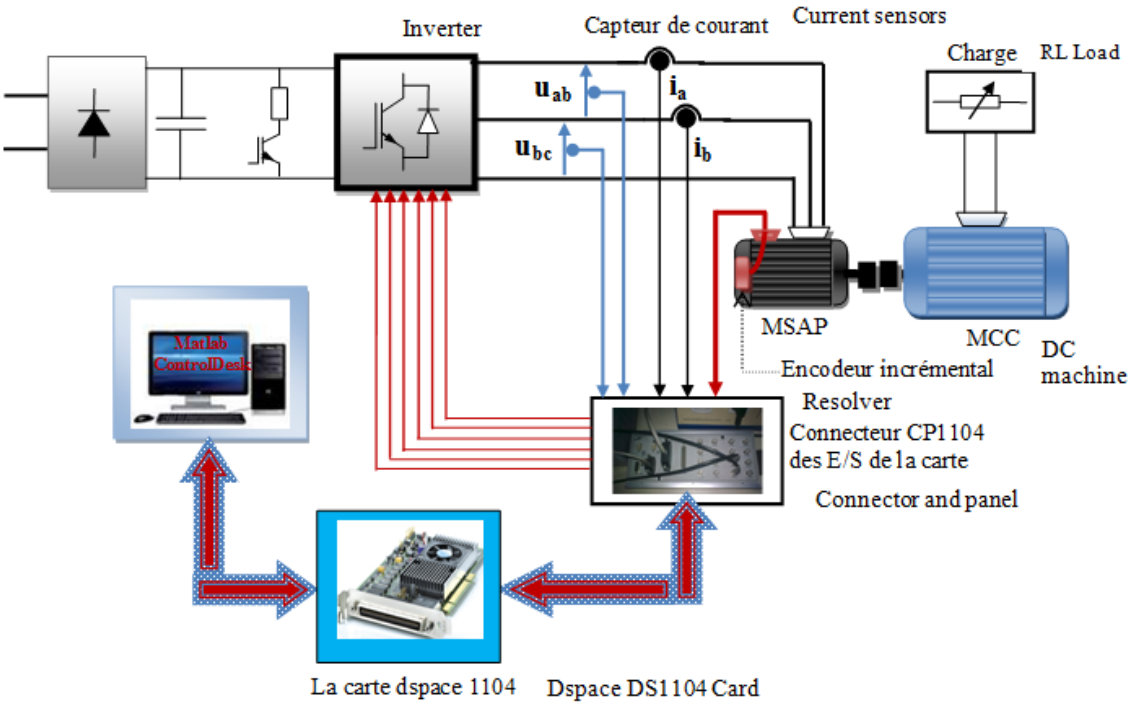

Figure 16. Laboratory setup block diagram

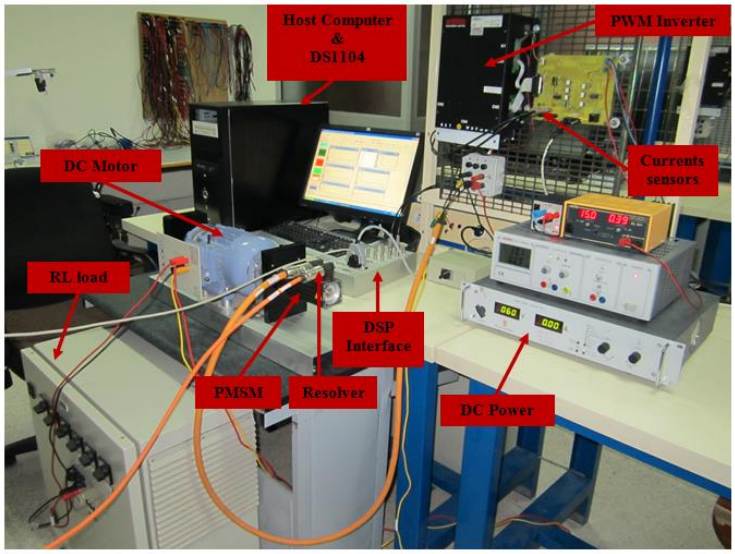

Figure 17. Laboratory setup (laboratory test bench)

In order to examine the performances of the classical and proposed DTC, the same tests were applied for each control strategy, which are: Speed tracking at no load, load torque variation atconstant speed and speed tracking at load torque. Figures 19, 21 and 23 show thatthe torque and flux ripples are greately reduced under the proposed DTC when compared to classical DTC (Figures18, 20 and 22) for various operating conditions within the speed/torque plan. In addition, the dynamic performance of these strategies are very similar. Indeed, Figure 24 shows that the speed and torque response time are very similar to that presented in Figure 25, respectively.

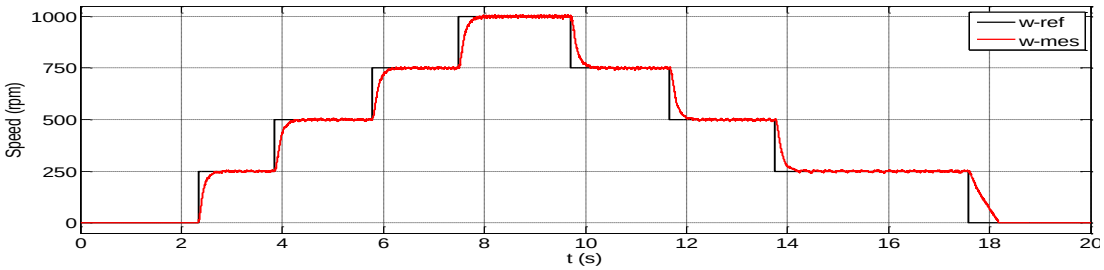

Figure 18a. Reference (w-ref) and measured speed (w-mes)

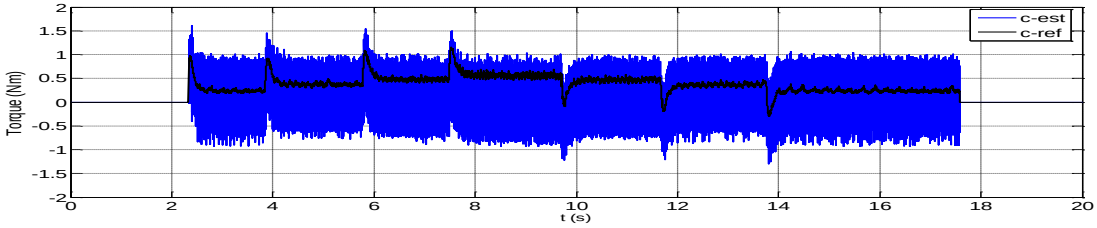

Figure 18b. Reference (c-ref) and estimated torque (c-est**)**

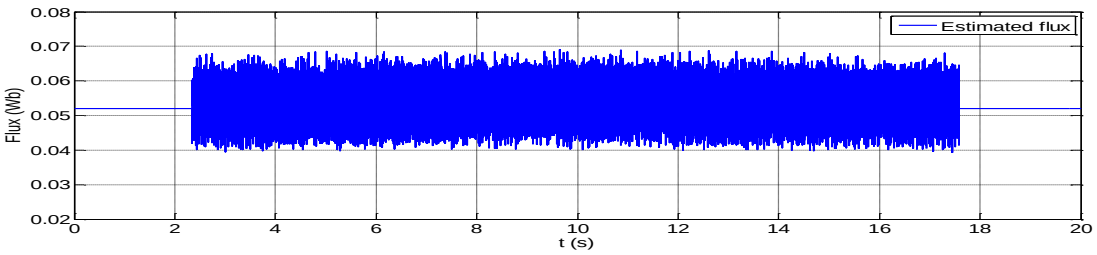

Figure 18c. Estimated stator flux linkage

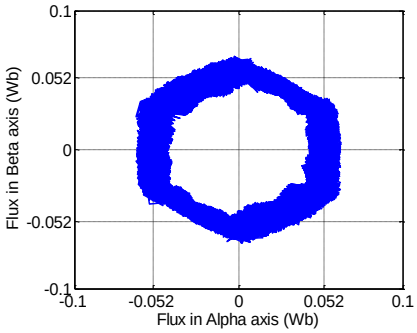

Figure 18d. Estimated stator flux vector components in (α,β) axis

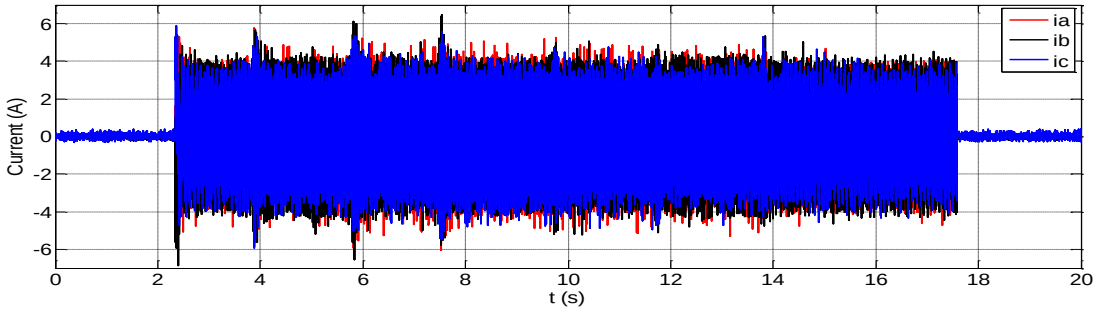

Figure 18e. Measured stator currents

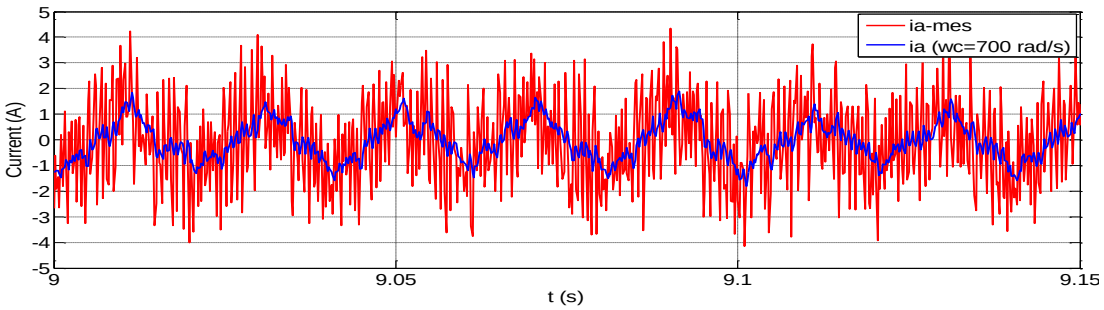

Figure 18f. Zoom in measured phase current (ia-mes), with and without low-pass filter (wc=700 rad/s)

Figure 18. No load experimental results of DTC. Measured speed and electromagnetic torque tracking performance, stator flux and currents waveforms

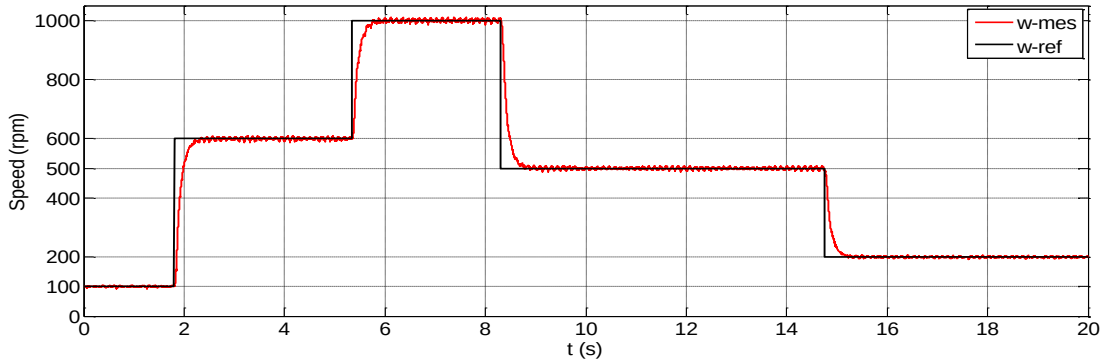

Figure 19a. Reference (w-ref) and measured speed (w-mes)

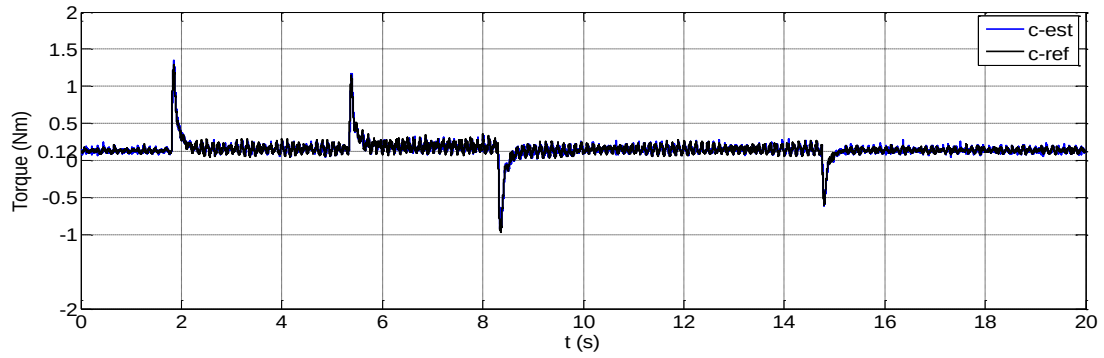

Figure 19b. Reference (c-ref) and estimated torque (c-est)

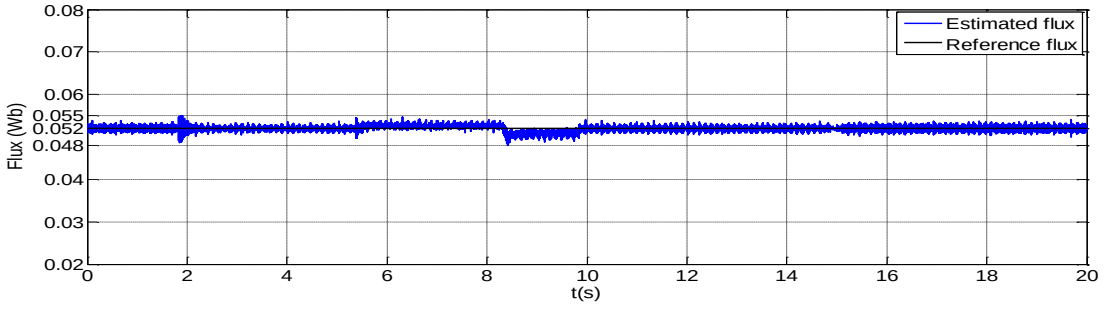

Figure 19c. Reference and estimated stator flux linkage

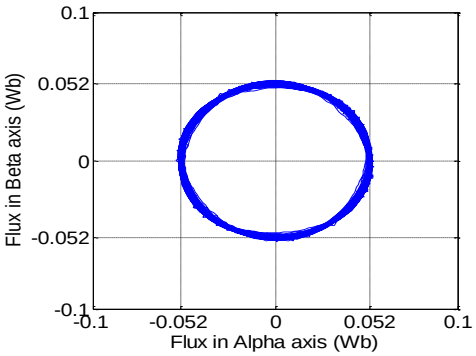

Figure 19d. Estimated stator flux vector components in (α,β) axis

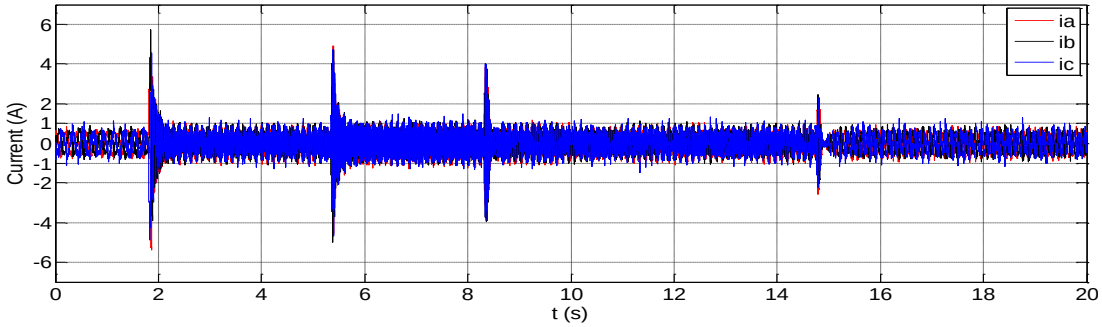

Figure 19e. Measured stator currents

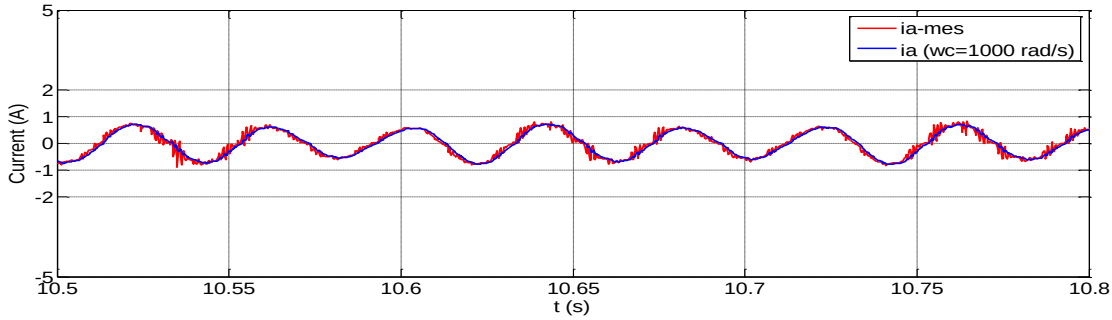

Figure 19f. Zoom in measured phase current (ia-mes), with and without low-pass filter (wc=1000 rad/s)

Figure 19. No load experimental results of CSF-DTC. Measured speed and electromagnetic torque tracking performance, stator flux and currents waveforms

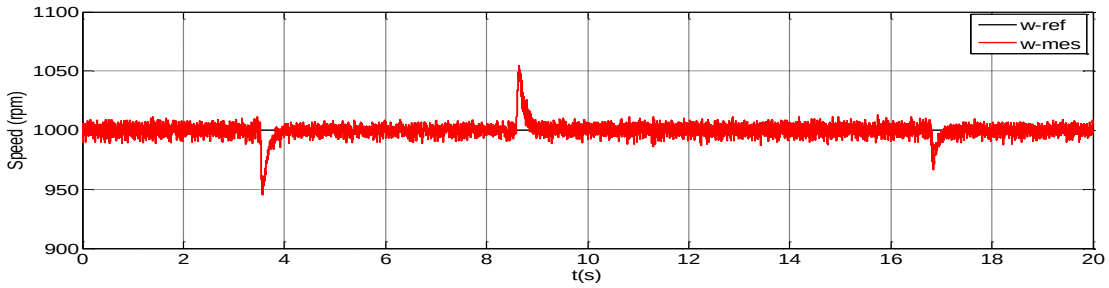

Figure 20a. Reference (w-ref) and measured speed (w-mes)

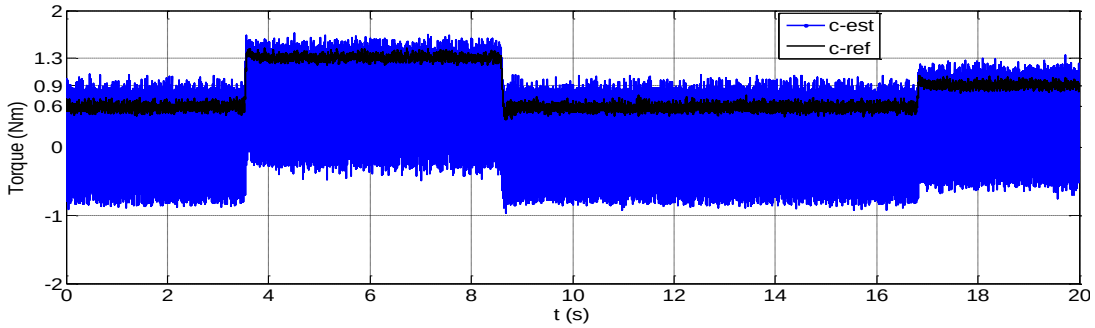

Figure 20b. Reference (c-ref) and estimated torque (c-est)

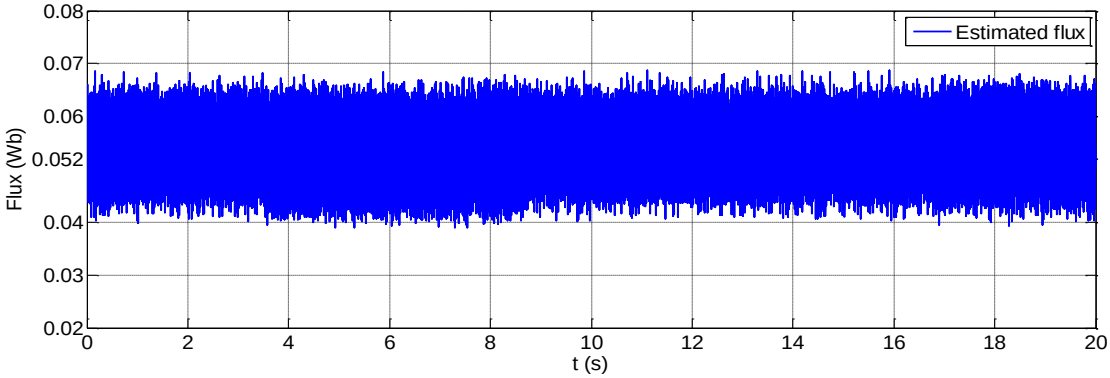

Figure 20c. Estimated stator flux linkage

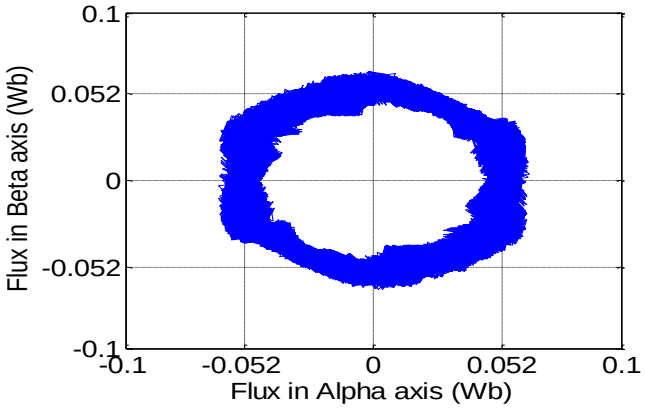

Figure 20d. Estimated stator flux vector components in (α,β) axis

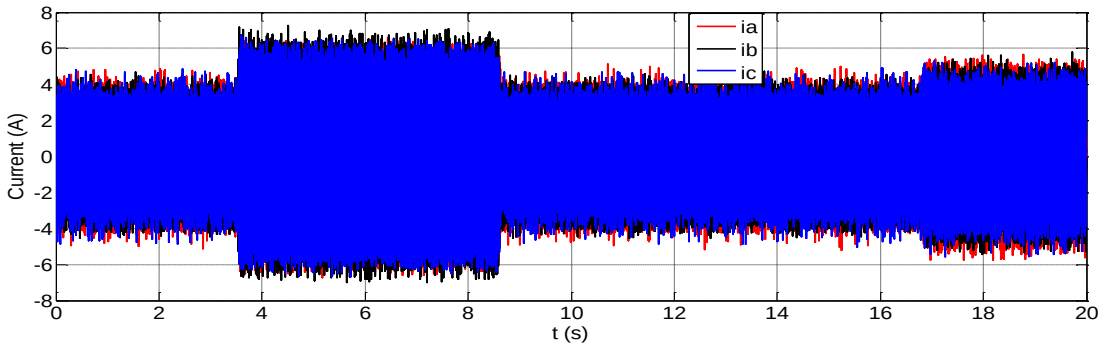

Figure 20e. Measured stator currents

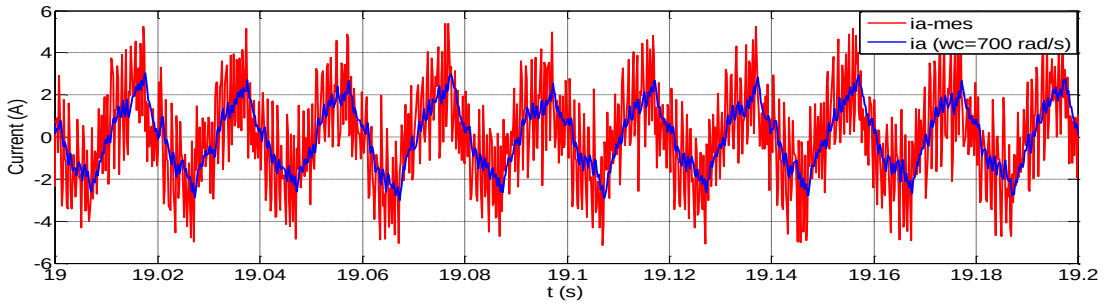

Figure 20f. Zoom in measured phase current (ia-mes), with and without low-pass filter (wc=700 ras/s)

Figure 20. Experimental results of DTC under various load torque values at 1000 rpm. Measured speed and electromagnetic torque tracking performance, stator flux and currents waveforms

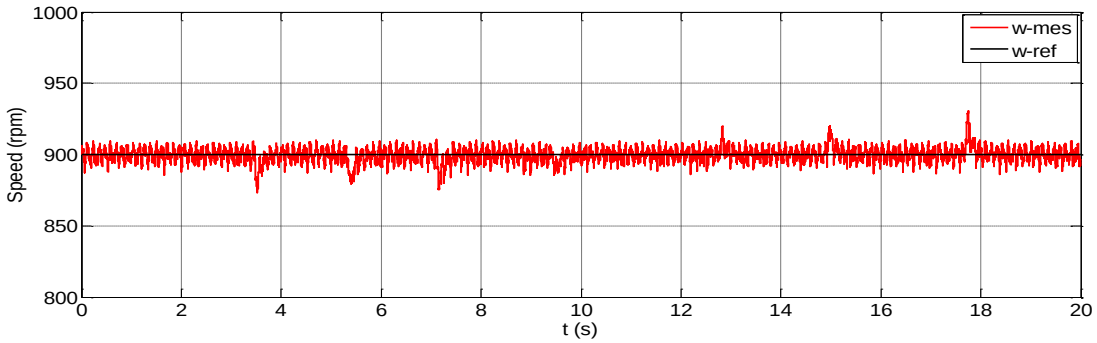

Figure 21a. Reference (w-ref) and measured speed (w-mes)

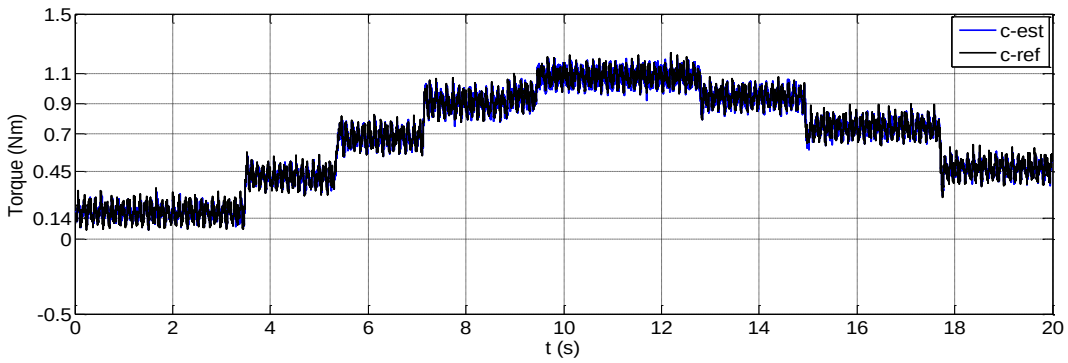

Figure 21b. Reference (c-ref) and estimated torque (c-est)

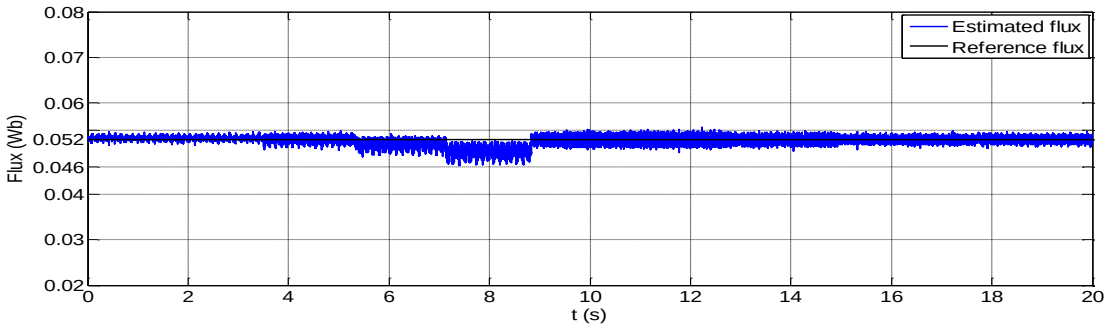

Figure 21c. Reference and estimated stator flux linkage

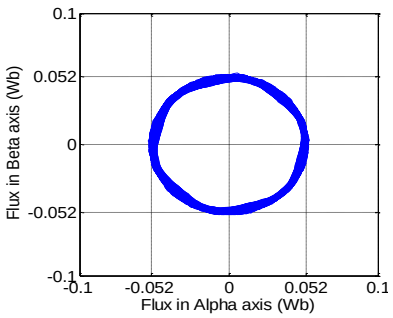

Figure 21d. Estimated stator flux vector components in (α,β) axis

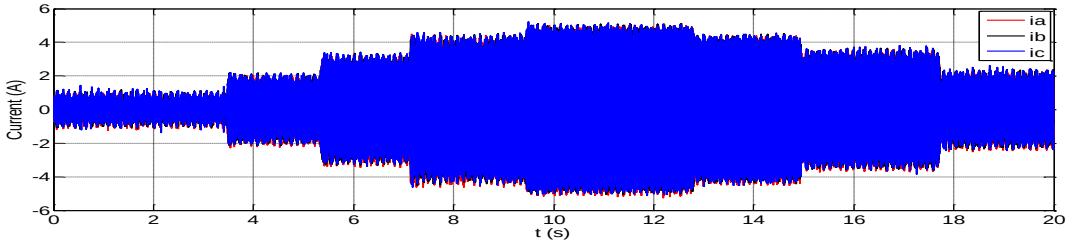

Figure 21e. Measured stator currents

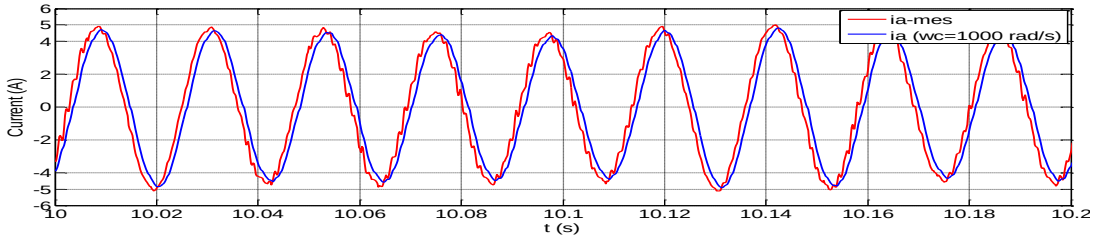

Figure 21f. Zoom in measured phase current (ia-mes), with and without low-pass filter (wc=700 ras/s)

Figure 21. Experimental results of DTC-SVM under various load torque values at 900 rpm. Measured speed and electromagnetic torque tracking performance, stator flux and currents waveforms

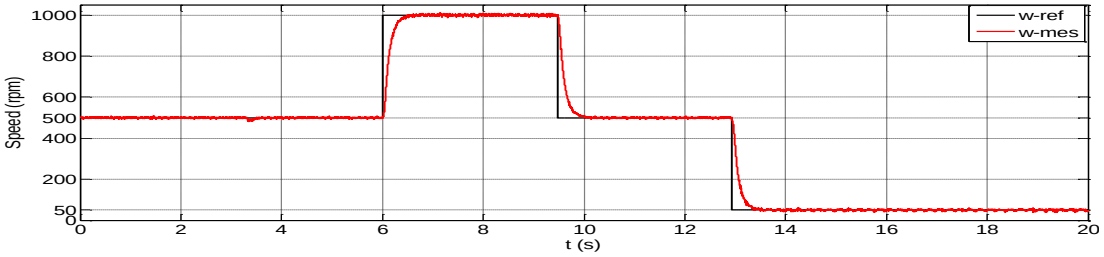

Figure 22a. Reference (w-ref) and measured speed (w-mes)

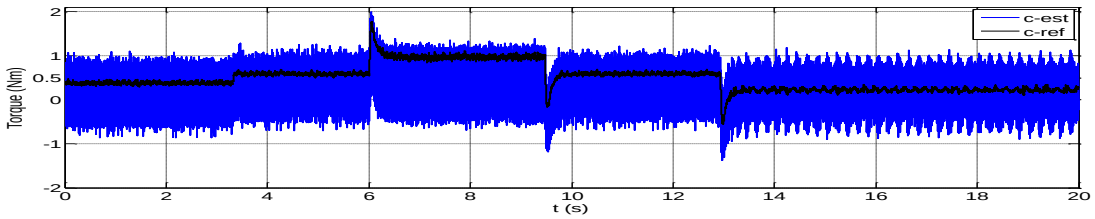

Figure 22b. Reference (c-ref) and estimated torque (c-est)

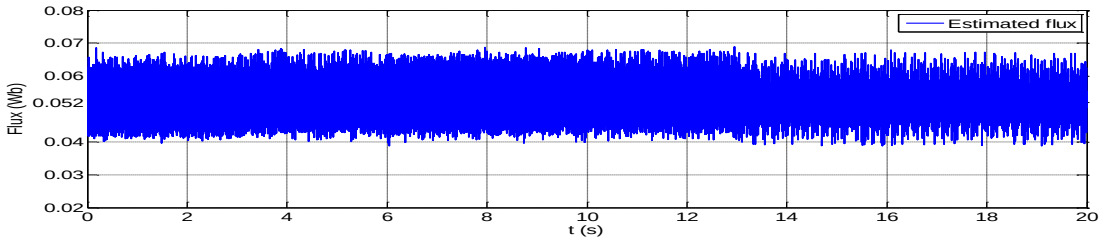

Figure 22c. Estimated stator flux linkage

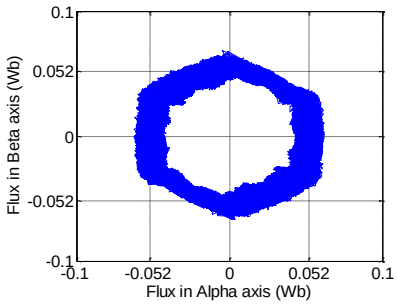

Figure 22d. Estimated stator flux vector components in (α,β) axis

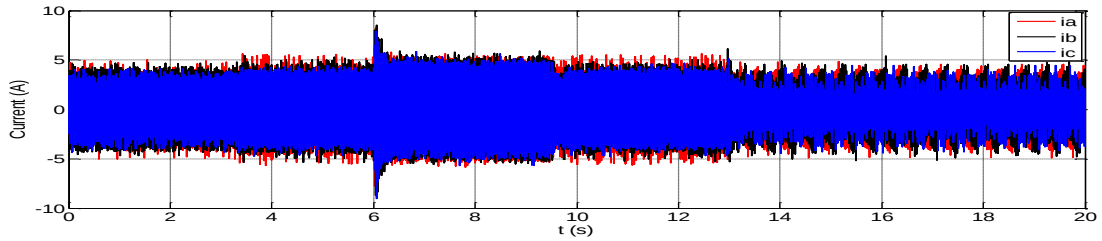

Figure 22.e. Measured stator currents

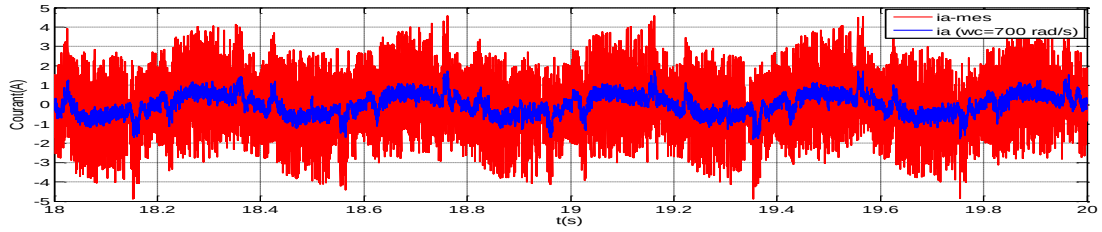

Figure 22.f. Zoom in measured phase current (ia-mes), with and without low-pass filter (wc=700 ras/s)

Figure 22. Experimental results of DTC under various speed set-pints with load torque. Measured speed and electromagnetic torque tracking performance, stator flux and currents waveforms

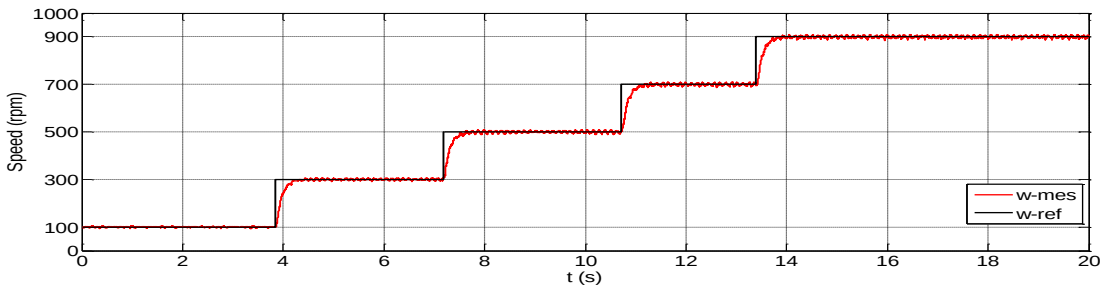

Figure 23.a. Reference (w-ref) and measured speed (w-mes)

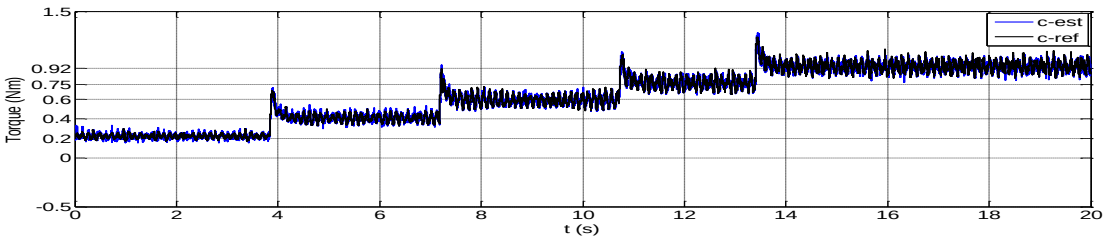

Figure 23b. Reference (c-ref) and estimated torque (c-est)

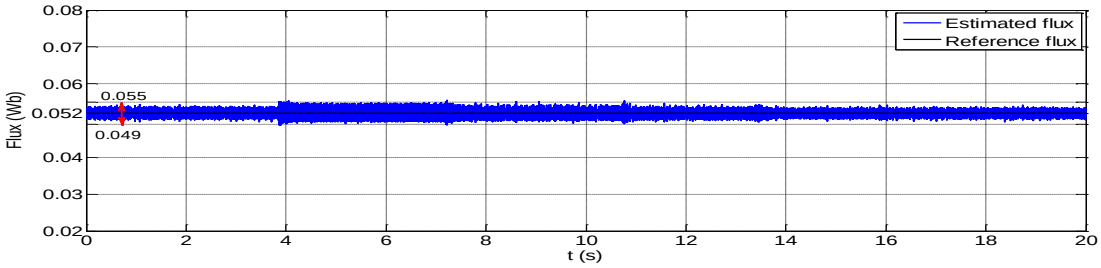

Figure 23c. Estimated stator flux linkage

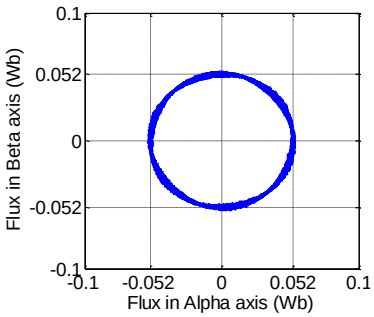

Figure 23d. Estimated stator flux vector components in (α,β) axis

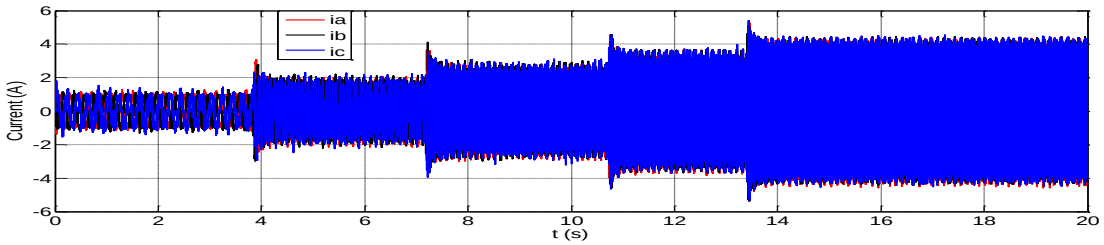

Figure 23e. Measured stator currents

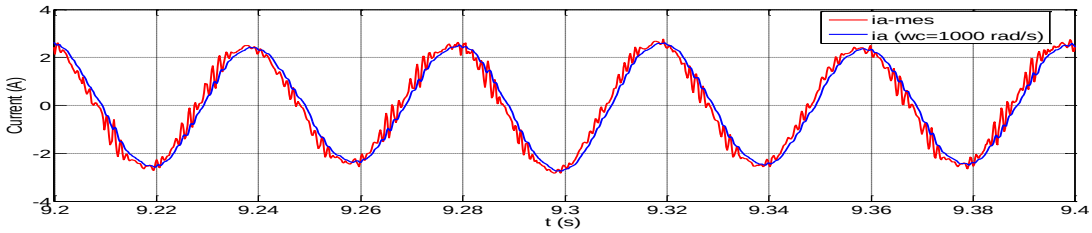

Figure 23f. Zoom in measured phase current (ia-mes), with and without low-pass filter (wc=700 ras/s)

Figure 23. Experimental results of DTC-SVM under various speed set-pints with load torque. Measured speed and electromagnetic torque tracking performance, stator flux and currents waveforms

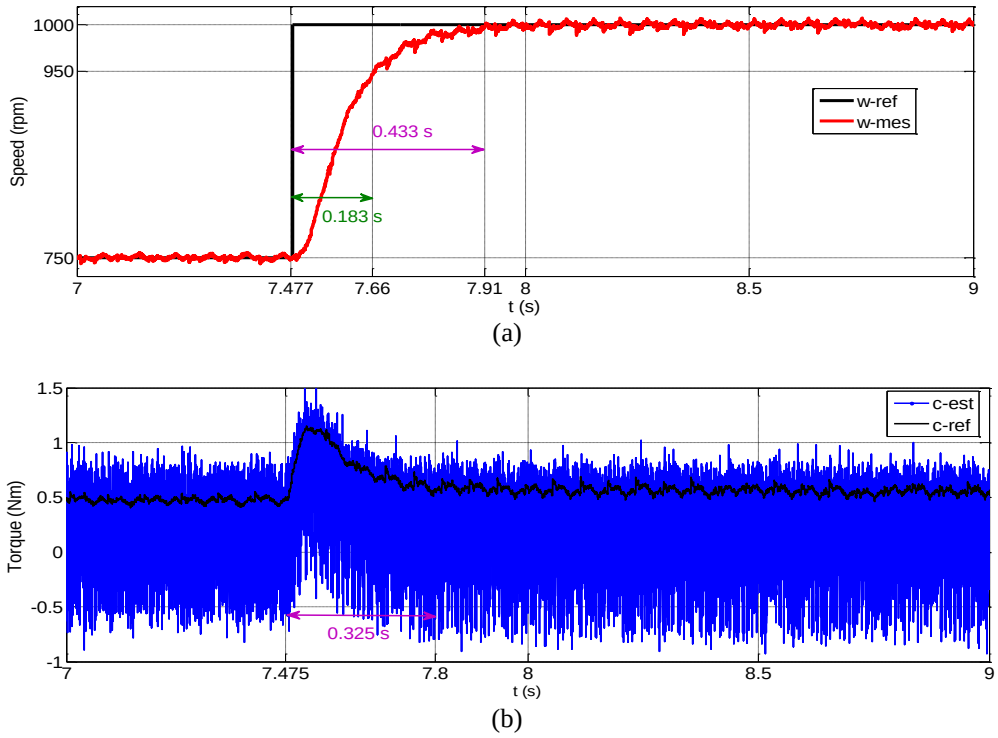

Figure 24. Speed (a) and torque (b) dynamic performance in case of DTC at no load

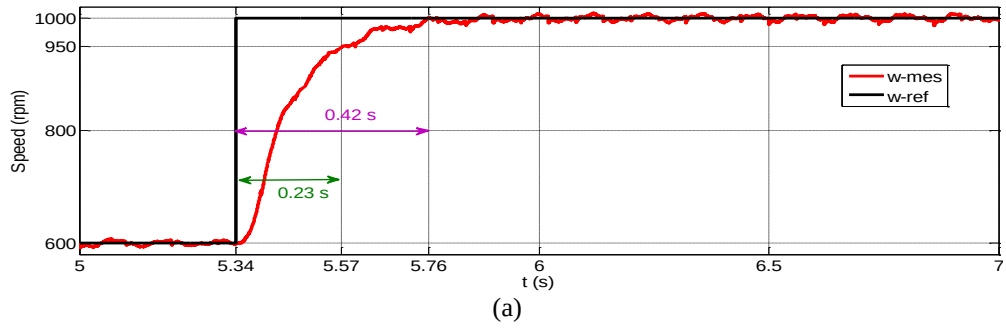

Figure 25. Speed (a) and torque (b) dynamic performance in case of DTC-SVM at no load

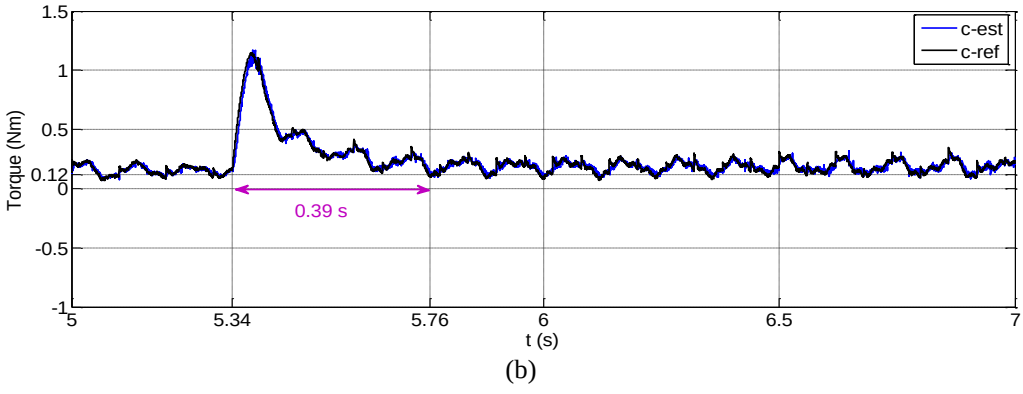

Figure 25. Speed (a) and torque (b) dynamic performance in case of DTC-SVM at no load

6. CONCLUSION

A robust constant switching frequency DTC using low switching losses SVM for PMSM drive has been proposed and validated in Matlab/Simulink and in DS1104 board. The simulation results confirm that, in spite of lower sampling time, both torque and flux ripples obtained with the modified DTC are greatly reduced when compared with those of the basic DTC.Also, the experimental torque and flux ripples are agree with the simulation results. In addition, the simulation and experimental results confirm that the studied control strategies ensure a fast dynamic response and very good decoupling in torque and stator flux control. Additionnaly, the studied schemes use an Integral and Proportional controllerswhich guaranteed a good disturbance rejection in speed, torque and flux closed loops. On the other hand, the asymmetrical SVM technique, proposed and validated based on the theoretical analysis, guarantee a constant switching frequency and reduce the power losses in the inverter.

REFERENCES

[1] S. Arumugam and M. Thathan " Novel Switching Table for Direct Torque Controlled Permanent Magnet Synchronous Motors to Reduce Torque Ripple *''Journal of Power Electronics, Vol. 13, No. 6, pp.939 – 954, November 2013.*

[2] R. Doktorska" Direct Torque Control with Space Vector Modulation (DTC-SVM) of Inverter-Fed Permanent Magnet Synchronous Motor Drive '' *PhD Thesis, Faculty of Electrical Engineering, Institute of Control and Industrial Electronics, 2005.*

[3] D. Casadei, F. Profumo, G. Serra andA. Tani " FOC and DTC: Two Viable Schemes for Induction Motors Torque Control '' *IEEE Transactions on Power Electronics, Vol. 17, No. 5, pp. 779 – 787, September 2002.*

[4] L. Lianbing, W. Xiaojun and S. Hexu " A Variable Voltage Direct Torque Control Based on DSP in PM Synchronous Motor Drive '' *Proceedings of IEEE TENCON, 2002*.

[5] K. Chikh, M. Khafallah, A. Saad and D. Yousfi " PMSM Vector Control Performance Improvement by Using Pulse with Modulation and Anti-windup PI Controller '' *Proceedings of IEEE : ICMCS'11 International Conference on Multimedia Computing and Systems, pp. 1–7, Ouarzazate, Morocco, April 2011, ISBN 978-1-61284-730-6.*

[6] K. Chikh, M. Khafallah, A. Saad and D. Yousfi " Drive with Low Torque and Flux Ripple for PMSM by Using Direct Torque Control with Space Vector Modulation '' *Proceedings of WASET: ICCESSE'11 International Conference on Computer, Electrical, and Systems Sciences, and Engineering, pp. 1130– 1137, Paris, France, June 2011, ISSN 2010-3778.*

[7] K. Chikh, M. Khafallah, A. Saad, D. Yousfi and H. Chaikhy " A Novel Fixed-Switching-Frequency DTC for PMSM Drive with Low Torque and Flux Ripple Based on Sinusoidal Pulse with Modulation and Predictive Controller '' *Proceedings of IEEE : ICMCS'12 International Conference on Multimedia Computing and Systems, pp. 1069– 1075, Tangier, Morocco, May 2012, ISBN 978-1-4673-1518-0.*

[8] K. Chikh, M. Khafallah and A. Saad " Improved DTC Algorithms for Reducing Torque and Flux Ripples of PMSM Based on Fuzzy Logic and PWM Techniques '' *INTECH Book entitled : Matlab - A Fundamental Tool for Scientific Computing and Engineering Applications, Vol. 1, Chapter 8, pp. 168 – 194, September 2012.*

[9] L. Tang, L. Zhong, M. F. Rahman and Y. Hu "A Novel Direct Torque Control for Interior Permanent-Magnet Synchronous Machine Drive with Low Ripple in Torque and Flux-a Speed-Sensorless Approach'' *IEEE Transactions on Industry Applications, Vol.39, pp. 1748-1756, No.6, Nov, 2003.*

[10] D. Swierczynski, M.Kazmierkowski and F. Blaabjerg " DSP based Direct Torque Control of permanent magnet synchronous motor (PMSM) using space vector modulation (DTC-SVM) '' *International Symposium on Industrial Electronics (ISIE). Vol.3, pp. 723 – 727, November 2002.*

[11] T. J. Vyncke, R. K. Boel and J. A. A. Melkebeek " Direct Torque Control of permanent magnet synchronous motors- an Overview '' *3rd IEEE Benelux Young Researchers Symposium in Electrical Power Engineering, Belgium , pp. 01 – 05, April 2006.*

[12] H. Ziane, J. M. Retif and T. Rekioua " Fixed-Switching-Frequency DTC Control for PM Synchronous Machine with Minimum Torque Ripples '' *Canadian Journal of Electrical and Computer Engineering, Vol. 33, No. 3/4, pp. 183 – 189, December 2008.*

[13] L. Zhong, M. F. Rahman, W. Y. Hu and K. W. Lim and M. A. Rahman " A Direct Torque Controller For Permanent Magnet Synchronous Motor Drives'' *IEEE Transactions on Energy Conversion, Vol. 14, No. 3, pp. 637 – 642, September 1999.*

[14] A. Ouarda and F. Ben Salem " Induction Machine DTC-SVM : A Comparison Between Two Approaches '' *10th International Multi-Conference on Systems, Signals & Devices (SDD), Tunisia, Hammamet, pp. 1 – 7, March2013.*

[15] E. Ozkop and H. I. Okumus " Direct Torque Control of Induction Motor Using Space Vector Modulation (SVM-DTC) '' *12th International Middle-East Power System Conference (MEPCON), Aswan, pp. 368 – 372, March 2008.*

[16] A. Sikorski et all " A Comparison of Properties of Direct Torque and Flux Control Methods (DTC-SVM, DTC-δ, DTC-2x2, DTFC-3A) '' *The International Conference on Computer as a Tool(EUROCON), Warsaw, pp. 1733 – 1739, September 2007.*

[17] D. Sun, Z. He, Y. He and Y. Guan " Four-Switch Inverter Fed PMSM DTC with SVM approach for Fault Tolerant operation '' *IEEE International Conference on Electrical Machines & Drives (IEMDC), Antalya, pp. 295 – 299, May 2007.*
[18] Y. Wan et all" A New Robust DTC-SVM for High Performance Induction Machine Drives '' *2nd International Symposium on Systems and Control in Aerospace and Astronautics (ISSCAA), Shenzhen, pp. 1-5, December 2008.*
[19] A. Trentin, P. Zanchetta, R. Wood and W. Typon" Performance Assessment of SVM Modulation Techniques for Losses Reduction in Induction Motor Drives '' *42ndIAS Annual Meeting Indystry Applications Conference, New Orleans.LA, pp. 1031 – 1037, September 2007.*
[20] P. J. P. Perruchoud and P. J. Pinewski " Power Losses for Space Vector Modulation Techniques'' *IEEE Power Electronics in Transportation Conference, pp. 167 – 173, October 1996.*
[21] Z. Sun et all " Research of the Influence of Different PWM Inverters on the Iron Losses for Induction Motors '' *17thInternational Conference on Electrical Machines and Systems (ICEMS), Hangzhou, China, pp. 96 – 100, October 2014.*
[22] C. Y. Leong et all " Research of the Influence of Different PWM Inverters on the Iron Losses for Induction Motors '' *International Conference on Power Electronics and Drives Systems (PEDS), Vol. 2, Kuala Lumpur, Malaysia, pp. 1123 – 1128,2005.*
[23] C. Ortega et all " Improved Waveform Quality in the Direct Torque Control of Matrix-Converter-Fed PMSM Drives '' *IEEE Transactions on Industrial Electronics, Vol. 57, No. 6, pp. 2101 – 2110, June 2010.*

BIOGRAPHIES OF AUTHORS

Khalid Chikh was born in Morocco in 1982. He received the Master's degree in electrical engineering from the Faculty of Science Semlalia in 2007, Marrakech, Morocco; and the Phd degree in electrical engineering in 2013 from the National Higher School of Electricity and Mechanics (ENSEM), Hassan II University, Casablanca, Morocco. Since Febrary 2014, he has been with Sultan Moulay Slimane University-EST, Morocco, where he is currently professor at the Electrical Engineering Department. His current research interests are in the application of power electronics converters, motor drives, intelligent and digital control using the DSP implementations, renewable energy and energy storage.

Abdallah Saad was born in Morocco in 1956. He received the Engineer and Doctor of Engineering degrees from National Polytechnic Institute of Grenoble-France-respectively in 1980 and 1982. From 1982 to 1986, he was Researcher at French National Center for Scientific Research (CNRS)-Electrostatics and Dielectric Materials Laboratory-Grenoble. After receiving the Doctor of Physical Sciences degree in 1986, he joined Hassan II University of Morocco. Professor of electrical engineering, he has several scientific and educational responsibilities. His main fields of interest are High Voltage and Electrical Insulations, modeling and control, renewable energy integration.

Mohamed Khafallah was born in Morocco in 1964. He received B.Sc., M.Sc. and Doctorate degrees from Hassan II University, Casablanca II, in 1989, 1991 and 1995 respectively, all in Electrical Engineering. In 1995 he joined the Department of Electrical Engineering at the National Higher School of Electricity and Mechanics (ENSEM), Hassan II University, Casablanca. His current research interests are in the application of power electronics converts and motor drives.

Driss Yousfi was born in Oujda, Morocco, in 1970.He received the B.S. and M.S. degrees in Electrical Engineering from Fes University, Morocco, respectively, in 1994 and 1996, and the Ph.D. degree in Electrical Engineering from place Oujda University, in 2001. From 1997 to 2001 he was a member of.the Electrical Engineering Laboratory at the High National School of Electrical and Mechanical Engineering, Morocco, working on the Modeling and Sensorless Control of Synchronous Motors. Since November 2001, he has been with Marrakech University-ENSA, Morocco, where he is currently professor at the Electrical Engineering Department and Staff Member of Control Systems, Power Electronics and Electric Drives "CSPEED" Group. Dr. Yousfi is a Member of the IEEE Industry Applications, IEEE Industrial Electronics, and IEEE Power Electronics Societies. His main research interests include sensorless control of Permanent Magnet Synchronous Machine, power converters and motor drives for electric traction systems, and DSP-based systems for real-time control.